Published in final edited form as:
Biochem J. 2010 August 15; 430(1): 69–78. doi:10.1042/BJ20091193.

Modulation of mammary cancer cell migration by 15-deoxy-$\Delta^{12,14}$-prostaglandin J_2: implications for anti-metastatic therapy

Anne R. Diers[1,4], **Brian P. Dranka**[1,4], **Karina C. Ricart**[1,4], **Joo Yeun Oh**[1,4], **Michelle S. Johnson**[1,4], **Fen Zhou**[1,4], **Manuel A. Pallero**[1], **Thomas M. Bodenstine**[1], **Joanne E. Murphy-Ullrich**[1,2,6], **Danny R. Welch**[1,2,3,5], and **Landar Aimee**[1,4,5]

[1]Department of Pathology, University of Alabama at Birmingham, Birmingham, AL 35294-0022

[2]Department of Cell Biology, University of Alabama at Birmingham, Birmingham, AL 35294-0022

[3]Department of Pharmacology/Toxicology, University of Alabama at Birmingham, Birmingham, AL 35294-0022

[4]Center for Free Radical Biology, University of Alabama at Birmingham, Birmingham, AL 35294-0022

[5]Comprehensive Cancer Center, University of Alabama at Birmingham, Birmingham, AL 35294-0022

[6]BioMatrix Engineering and Regenerative Medicine Center, University of Alabama at Birmingham, Birmingham, AL 35294-0022

SYNOPSIS

Recently, a number of steps in the progression of metastatic disease have been shown to be regulated by redox signaling. Electrophilic lipids affect redox signaling through the post-translational modification of critical cysteine residues in proteins. However, the therapeutic potential as well as the precise mechanisms of action of electrophilic lipids in cancer cells is poorly understood. In this study, we investigate the effect of the electrophilic prostaglandin 15-deoxy-$\Delta^{12,14}$-prostaglandin J_2 (15d-PGJ_2) on metastatic properties of breast cancer cells. 15d-PGJ_2 was shown to decrease migration, stimulate focal adhesion disassembly and cause extensive F-actin reorganization at low concentrations (0.03-0.3 μM). Importantly, these effects seem to be independent of PPARγ and modification of actin or Keap1, which are known protein targets of 15d-PGJ_2 at higher concentrations. Interestingly, the p38 inhibitor SB203580 was able to prevent both 15d-PGJ_2-induced F-actin reorganization and focal adhesion disassembly. Taken together, our results suggest that electrophiles such as 15d-PGJ_2 are potential anti-metastatic agents which exhibit specificity for migration and adhesion pathways at low concentrations where there are no observed effects on Keap1 or cytotoxicity.

Keywords

Post-translational protein modification; thiol; redox signaling; focal adhesions; actin cytoskeleton; reactive lipid species

INTRODUCTION

Ninety percent of all cancer related deaths are the result of metastasis; thus understanding the regulation of this complex process is important in developing new anti-metastatic treatment strategies. It is becoming clear that a number of steps in the metastatic cascade are regulated

by redox signaling. The primary mechanism by which redox signaling occurs is through the

Corresponding author: Aimee Landar, Ph.D., Department of Pathology, University of Alabama at Birmingham, Biomedical Research Building II, 901 19th Street South, Birmingham, Alabama 35294, Tel: 205-975-9507, Fax: 205-934-1775, landar@uab.edu..

AUTHOR CONTRIBUTION

Anne Diers, Brian Dranka, Karina Ricart, Joo Yeun Oh, Michelle Johnson, Fen Zhou, Manuel Pallero, and Thomas Bodenstine performed experiments. Anne Diers, Fen Zhou, Joo Yeun Oh, Joanne Murphy-Ullrich, Danny Welch, and Aimee Landar designed experiments and analysed results. All authors contributed to the preparation of the manuscript.

[1]The abbreviations used are:

15d-PGJ$_2$	15-deoxy-$\Delta^{12,14}$-prostglandin J$_2$
BD-15d-PGJ$_2$	BODIPY-15-deoxy-$\Delta^{12,14}$-prostglandin J$_2$
BODIPY FL EDA	4,4-difluoro-5,7-dimethyl-4-bora-3a,4a-diaza-*s*-indacene-3-propionyl ethylenediamine
bt-15d-PGJ$_2$	biotin-15-deoxy-$\Delta^{12,14}$-prostglandin J$_2$
DAPI	4′,6-diamidino-2-phenylindole
EpRE	Electrophile Response Element
EtOH	Ethanol
FBS	Fetal bovine serum
GSH	Glutathione
HCl	Hydrochloric acid
H-Ras	Harvey rat sarcoma viral oncogene homolog
HRP	Horseradish peroxidase
Hsp27	Heat shock protein 27
Keap1	Kelch-like ECH-associated protein 1
MMP	Matrix metalloproteinase
NaBH4	Sodium borohydride
NaOH	Sodium hydroxide
NEM	*N*-Ethylmaleimide
NFkB	Nuclear factor kappa-light-chain-enhancer of activated B cells
Nrf-2	Nuclear factor erythroid 2-related factor 2
PBS	Phosphate buffered saline
PI	Propidium iodide
PMA	Phorbol 12-myristate 13-actetate
PPAR	Peroxisome proliferator-activated receptor
ROS	Reactive oxygen species
ROSI	Rosiglitazone
SDS	Sodium dodecyl sulfate
SPARC	Secreted protein acidic and rich in cysteine
TBS-T	Tris buffered saline with Tween 20
WASP	Wiskott-Aldrich Syndrome protein
WAVE	WASP verprolin homologous protein

post-translational modification of critical cysteine residues (thiols) in redox-sensitive proteins. The modification of thiols in proteins such as peroxisome proliferator-activated receptor gamma (PPARγ), actin, Keap1, and H-Ras can change the protein structure and/or function of these target proteins and thereby alter signaling pathways [1-5]. Known downstream effects of modification of redox-sensitive signaling pathways include modulation of matrix metalloproteinase (MMP) expression [6], NFκB regulated gene expression, and mitochondrial reactive oxygen species (ROS) generation [7-10], and activity of these pathways has been shown to be directly linked to metastatic potential in multiple cancer types [7,11-13]. Taken together, these studies suggest there are redox-sensitive signaling pathways controlling basic processes required for metastasis.

Species capable of modifying redox signaling pathways can be derived from several sources such as the diet, environment, or endogenously through enzymatic or non-enzymatic processes [14,15]. One such redox signaling molecule is the electrophilic cyclopentenone prostaglandin, 15-deoxy-$\Delta^{12,14}$-prostaglandin J_2 (15d-PGJ_2) which modifies primarily cysteine residues through a Michael-type addition [16]. In the context of cancer, 15d-PGJ_2 has garnered much interest because of its ability to inhibit angiogenesis, cause growth arrest, and induce cell death in several cancer cells lines [17-20]. Interestingly, although 15d-PGJ_2 has been shown to be cytotoxic in cancer cells, little is known about its effects on metastasis.

There are two basic mechanisms that have been described to explain the biological actions of 15d-PGJ_2. First, 15d-PGJ_2 has been proposed as the endogenous ligand for PPARγ. PPARs are ligand-inducible transcription factors which belong to the nuclear hormone receptor super-family [21,22]. New evidence suggests they may also play a role in oncogenesis, as they modulate proliferation and apoptosis and are expressed in many human tumors including breast [23]. The second mechanism of action by which 15d-PGJ_2 alters cellular signaling pathways is through the post-translational modification of redox-sensitive signaling molecules as mentioned above. There are multiple protein targets of 15d-PGJ_2 which can mediate diverse biological responses. We have termed this group of proteins the electrophile responsive proteome [24]. This latter mechanism likely underlies the pleiotropic effects of 15d-PGJ_2 reported in the literature [25].

Cellular migration plays an important role in metastasis, and 15d-PGJ_2 has been shown to inhibit migration [26,27]. There is also evidence demonstrating that 15d-PGJ_2 alters cytoskeletal structure in multiple cell types including neuroblastoma and mesangial cells; however, these studies reported cytotoxicity associated with cytoskeletal alterations [2,3]. The cytoskeletal effects of 15d-PGJ_2 have been largely attributed to the direct modification of proteins such as actin, vimentin, and tubulin [2,3]. In this study, we investigated the effects of 15d-PGJ_2 on the F-actin cytoskeleton at lower concentrations which do not cause cytotoxicity. The effect of 15d-PGJ_2 on the cytoskeleton and migration might have important implications in the inhibition of metastatic processes such as invasion, intravasation, and extravasation.

The goals of this study were to determine the effects of non-toxic, low concentrations of 15d-PGJ_2 on regulation of cytoskeletal organization and its influence on cell migration and to determine the mechanism of action of 15d-PGJ_2 at these low concentrations. We first investigated the effect of 15d-PGJ_2 on cell viability, migration, and focal adhesion disassembly. In addition, we determined the effects of 15d-PGJ_2 on F-actin cytoskeletal structure and examined the roles of direct actin adduction, PPARγ activation, and redox signaling pathways in 15d-PGJ_2 mediated cytoskeletal regulation. Our study is the first to demonstrate that 15d-PGJ_2 can alter actin organization with minimal direct adduct formation with actin, and that this effect coincides with decreased migration and increased focal adhesion disassembly. These results suggest a role for redox signaling pathways, rather than direct cytoskeletal disruption in the mechanism of 15d-PGJ_2 in cancer cells.

MATERIALS AND METHODS

Materials

BODIPY FL EDA was purchased from Molecular Probes (Eugene, OR). Alexa Fluor® 633 Phalloidin was purchased from Invitrogen (Carlsbad, CA). 15d-PGJ_2, prostaglandin E_2, 15(R)-PGD_2, and Rosiglitazone were purchased from Cayman Chemical (Ann Arbor, MI). The p38 inhibitor SB203580 was purchased from Calbiochem (San Diego, CA). BODIPY FL EDA tagged 15d-PGJ_2 (BD-15d-PGJ_2) was synthesized using the method previously described by Landar et al. [28]. EZ-link 5-(biotinamido)pentylamine was purchased from Pierce (Rockford, IL) for the synthesis of biotinylated 15d-PGJ_2 (bt-15d-PGJ_2) as previously described [4]. Structures of the parent compound, 15d-PGJ_2, and tagged derivatives are shown in Figure 1. It was determined that tagging 15d-PGJ_2 does not affect its biological activity by comparing the effect of tagged and untagged analogs on migration, colony formation, and the F-actin cytoskeleton (Supplementary Figure 1). Additionally, the BODIPY fluorophore itself does not alter any of the biological effects examined (Supplementary Figure 1). All other reagents used were of analytical grade.

Cell culture

JC mouse mammary adenocarcinoma cells (ATCC, Manassas, VA) were cultured in RPMI 1640 media (Mediatech, Manassas, VA) supplemented with 10% fetal bovine serum (FBS; Atlanta Biologicals, Atlanta, GA). Cultures were maintained in 5% CO_2 and humidified in a 37°C incubator. All experiments were performed at 0.5% FBS in RPMI 1640 media at ~50% confluence.

Assessment of cell viability

Cell viability was assessed using two different methods. Apoptosis and necrosis were measured after treatment with the indicated concentrations of 15d-PGJ_2 for 16 h by flow cytometric analysis using an Annexin V FITC Apoptosis Detection Kit (Calbiochem). Briefly, treated cells were trypsinized and then incubated with Annexin V FITC and propidium iodide (PI). Gating parameters were set using PI only, Annexin V only, and no staining controls, and 10,000 events were collected for each experimental sample. Cells staining positive for both PI and Annexin V were considered late apoptotic. Cells staining positive for PI only or Annexin V only were scored as necrotic or early apoptotic, respectively. Cells which stained negative for both PI and Annexin V were scored as viable cells. Fluorescence was measured using a BD LSR II flow cytometer. Colony formation was measured after treatment with indicated concentrations of 15d-PGJ_2 for 16 h. Cells from experimental dishes were trypsinized and collected. All cells from each dish were then centrifuged, resuspended in fresh medium, and counted. Cells were then plated in 6 well plates at low density (100-200 cells per well), and clones were allowed to grow for 14 days in complete medium in the presence of 0.1% gentamycin. Cells were then fixed with 70% ethanol and stained with Coomassie blue for analysis of colony formation as previously described [29].

Measurement of glutathione

JC cells were treated with 15d-PGJ_2 for 16 h at the concentrations indicated. Total glutathione (GSH; glutathione + glutathione disulfide) was determined in lysates as described previously [30]. Briefly, after treatment, cells were lysed in 10 μM DTPA containing 0.1% Triton X-100 in PBS, pH 7.4. Total glutathione was determined by monitoring the reduction of 5,5′-Dithio-bis(2-nitro-benzoic acid spectrophotometrically at 412 nm. Protein content was assayed by the Bradford method (Bio-Rad protein assay kit, Hercules, CA).

Fluorescence microscopy

Fluorescence microscopy was used to visualize phosphorylated FAK (p-FAK), and F-actin. JC cells were plated on glass coverslips, treated, and fixed using paraformaldehyde (3.7%) for 10 min. The cells were then rinsed twice with PBS and permeabilized with 0.1% Triton X-100 (v/v) in PBS. To determine the relative levels of p-FAK, samples were blocked with 5% normal goat serum (Vector Labs, Burlingame, VT) and 0.3% Triton X-100 (v/v) in PBS for 60 min at room temperature. Cells were then incubated in p-FAK (Tyr 397) antibody (Cell Signaling, Danvers, MA) at 1:100 in antibody dilution buffer (1% BSA (w/v) and 0.3% Triton X-100 (v/v) in PBS) overnight at 4°C. Alexa Fluor® 488 conjugated goat anti-rabbit secondary antibody (1:500, 1 h; Invitrogen) was applied, and then coverslips were then mounted on glass slides using Vectashield Hard Set Mounting Medium containing DAPI (Vector Laboratories). Phospho-FAK foci were visualized using confocal fluorescence microscopy on a Leica DMIRBE laser scanning confocal microscope with excitation from a 488 nm laser line and emission detection suitable for fluorescein. Nuclei were imaged using a UV laser line and emission detection suitable for DAPI.

To determine the extent of actin polymerization, JC cells were prepared as described above Next, cells were incubated with blocking solution (PBS containing 1% BSA, w/v) for 30 min followed by application of 2 units of Alexa Fluor® 633 Phalloidin (Invitrogen) for 30 min at room temperature in blocking solution. F-actin imaging was performed with a 633 nm laser line for excitation and emission detection suitable for Cy5. In p-FAK and F-actin co-staining experiments, Alexa Fluor® 633 Phalloidin was co-incubated with secondary antibody. All confocal images represent single sections and were manipulated using linear histogram correction in Adobe Photoshop CS3 (Adobe Systems Inc., San Jose, CA). Fluorescence quantification was performed using SimplePCI software (Hamamatsu Corporation, Sewickley, PA).

Determination of the modification of Keap1 and β-actin by 15d-PGJ_2

To determine the extent of modification of Keap1 by 15d-PGJ_2, JC cells were treated with increasing concentrations (0.3-20 μM) of bt-15d-PGJ_2 for 4 h. After the treatment, cell lysates were prepared in 1% Triton X-100 in Tris-HCl (10 mM) lysis buffer. Biotinylated proteins were affinity precipitated using 100 μL of a 50% slurry of Neutravidin beads (Pierce) which were pre-washed with 20 mM Tris-HCl (pH 7.4, 6 times). Cell lysates (6 mg protein) containing protease inhibitor cocktail were added to the beads and incubated for 3 h at room temperature with rotation. Beads were then washed with 600 μl 0.1 M glycine (pH 2.8, 6 times) followed by 600 μl 20 mM Tris Base (pH 10, 6 times) and then 600 μl 20 mM Tris-HCl (pH 7.4) to neutralize the beads. Samples were then prepared for analysis by heating the beads to 80°C for 10 min in 80 μl of 5x sample buffer (0.5 M Tris, 20% SDS, 50% Glycerol, 1% Bromophenol blue, pH 6.8) containing β-mercaptoethanol to release the biotin labeled proteins. Samples were centrifuged at 12,500 rpm for 10 min at 4°C, and supernatants used for analysis. Proteins were separated by SDS-PAGE, and transferred to nitrocellulose membranes at 100V for 2 h and then membranes blocked with 5% skim milk in TBS-T. Membranes were incubated with a polyclonal primary antibody against Keap1 (E-20 1:1000 dilution in 5% skim milk in TBS-T; Santa Cruz Biotechnology, Inc., Santa Cruz, CA), followed by a HRP (horseradish peroxidase)-conjugated donkey anti-goat secondary antibody (1:1000 dilution in 5% skim milk in TBS-T; Santa Cruz). Membranes were developed by chemiluminescence using SuperSignal West Dura substrate (Pierce) and sequential images taken with quantitation only performed on bands which had not reached saturation.

To determine the modification of β-actin by 15d-PGJ_2, JC cells were treated as described above. After treatment, cell lysates were prepared in *N*-Ethylmaleimide (NEM; Pierce) containing lysis buffer (10 mM NEM, 1% Triton X-100 in PBS) for 1 h in order to alkylate sulfhydryls

and prevent auto-oxidation during the sample processing. Beta-mercaptoethanol was added to quench the excess NEM. Cell lysates were incubated with sodium borohydride (10 mM $NaBH_4$ in 5 mM NaOH) overnight to reduce the carbonyl group on then pentene ring in order to stabilize the lipid adducts on proteins. Biotinylated proteins were affinity precipitated using 100 μL of a 50% slurry of Neutravidin beads (Pierce) which were pre-washed with 20 mM Tris-HCl (pH 7.4, 6 times). Cell lysates (3 mg protein) containing protease inhibitor cocktail were added to the beads and incubated for 3 h at room temperature with rotation. Proteins were separated by SDS-PAGE, and transferred to nitrocellulose membrane at 100V for 2 h and membranes blocked with 5% skim milk in TBS-T. Membranes were incubated with a polyclonal primary antibody against β-actin (Cell Signaling; 1:1000 dilution in 5% skim milk in TBS-T), followed by a HRP-conjugated donkey anti-rabbit secondary antibody (1:1000 dilution in 5% skim milk in TBS-T; GE Healthcare, Piscataway, NJ). Membranes were developed as described above.

Measurement of cellular migration

JC cells were grown to confluence in 6 well plates, and then scratched with the narrow end of a sterile pipet tip. Medium was immediately changed to remove floating cells and was replaced with media containing increasing concentrations of 15d-PGJ_2 or EtOH vehicle control. The width of the scratch was measured at four points in each well after initial wounding, and cells were incubated for 8 h at 37°C in a CO_2-incubator. After 8 h, the scratch width was measured again, and the ability of the cells to migrate into the cell-free zone (relative motility) was expressed as the normalized percent change in the width of the scratch after 8 h compared to EtOH control.

Focal adhesion disassembly assay

Focal adhesions were assessed using interference reflection microscopy. JC cells were plated on glass coverslips, allowed to attach and then grown 24 h before being serum starved (0.5% FBS RPMI 1640) for 30 min prior to indicated treatments. Cells were fixed in 3% glutaraldehyde (Sigma, St. Louis, MO) for 30 min at 37 °C and then rinsed and mounted on glass slides. Slides were imaged using interference reflection microscopy using a modified inverted Zeiss microscope as described previously [31]. Cells containing > 6 focal adhesions were scored as positive by an observer (MAP) without prior knowledge of sample conditions. 300 cells/coverslip were scored for each treatment group in triplicate.

Western blot analysis

Cell lysate proteins were resolved using SDS-PAGE and transferred to nitrocellulose membranes (Bio-Rad). Protein levels were quantified using the method of Bradford (Bio-Rad), and equivalent amounts of protein were loaded. Uniform protein loading was confirmed using Ponceau S staining of membranes and showed no significant differences protein levels on blots among samples. Membranes were blocked in 5% BSA (w/v) in TBS-T, and then incubated with primary antibodies overnight at 4°C. Antibody conditions were as follows: anti-FAK (1:1000; Cell Signaling), anti-phosphorylated-p38 (Cell Signaling; 1:1000), anti-p38 (Cell Signaling; 1:1000) and β-actin (1:1000; Cell Signaling). After washing with TBS-T, membranes were incubated with HRP-conjugated secondary antibody. Membranes were developed using SuperSignal West Dura chemiluminescence substrate (Pierce) and imaged using a CCD camera imaging system.

Statistical Analysis

Data were expressed as means ± standard error of the mean (SEM) at a minimum in triplicate, and subjected to Student's t-test or one-way analysis of variance (ANOVA) followed by

Bonferroni's multiple comparison tests. P values less than 0.05 were considered statistically significant.

RESULTS

15d-PGJ_2 toxicity in JC mouse mammary adenocarcinoma cells

15d-PGJ_2 has been shown to induce apoptotic cell death in a number of cancer cell lines at concentrations ranging from 5-50 μM [32-35]. In order to determine non-toxic concentrations of 15d-PGJ_2, cytotoxicity was assessed using PI and Annexin V-FITC co-staining measured by flow cytometry. JC cells were treated with 15d-PGJ_2 (0.01-3 μM) for 16 h. By this method, we are able to distinguish apoptotic and necrotic cell death. As seen in Figure 2A, at concentrations ranging from 0.01 to 3 μM, there are no significant changes in viability. Furthermore, there was no indication of apoptotic or necrotic cell death in response to 15d-PGJ_2 treatment as determined by the lack of cells staining positive for PI or Annexin V-FITC (data not shown). In contrast and consistent with reports in the literature [32-35], when JC cells are treated with higher concentrations (20 μM) of 15d-PGJ_2, there is a significant decrease in cell viability as well as an increase in both late apoptotic and necrotic cell populations (Supplementary Figure 2).

15d-PGJ_2 toxicity was also assessed using a colony formation assay. This assay measures the replicative ability of cells to form colonies after treatment, an important characteristic of cancer cells. Interestingly, when JC cells were treated with 15d-PGJ_2, a marked decrease in colony formation was measured at concentrations as low as 0.01 μM (Figure 2B). Taken together, these data suggest that treatment with low concentrations of 15d-PGJ_2 (0.01-3 μM) attenuates the clonogenic capacity of JC cells, but does not cause apoptosis or necrosis. Since re-adherence to tissue culture plates and proliferation are two critical steps for successful colony formation in this assay, these data also suggest that 15d-PGJ_2 may attenuate proliferation and/or adhesion pathways. Further investigation demonstrated that 15d-PGJ_2 does not cause alterations in cell cycle progression in this model; however, re-adherence of cells to tissue culture plastic after treatment with 15d-PGJ_2 and subsequent trypsinization was impaired (59.02% ± 9.79 of vehicle control treated cells, $p < 0.05$; data not shown). Therefore, we conclude 15d-PGJ_2 does not cause cell death at concentrations at or below 3 μM, and the decreased colony formation caused by 15d-PGJ_2 appears to be due to a decreased ability of cells to re-adhere after plating, rather than decreased cell viability *per se*.

15d-PGJ_2 attenuates migration

Having established sub-lethal concentrations of 15d-PGJ_2, we next examined the effect of this electrophile on cell motility using a scratch assay. Treatment with 15d-PGJ_2 caused a concentration-dependent decrease in cell migration over 8 h with significant changes seen at concentrations of 15d-PGJ_2 equal or greater than 0.03 μM (Figure 3). These results demonstrate that low, non-toxic concentrations of 15d-PGJ_2 attenuate cancer cell migration.

Effects of 15d-PGJ_2 on focal adhesion kinase signaling

Focal adhesion kinase (FAK) is a cytoplasmic protein tyrosine kinase whose expression has been shown to be frequently deregulated in cancer (reviewed in [36]). To investigate the potential role of FAK signaling in 15d-PGJ_2-induced attenuation of migration, we treated JC cells with 0.3 μM 15d-PGJ_2 for 30 min and 4 h, and determined total FAK protein levels. Treatment with this sub-lethal concentration of 15d-PGJ_2 did not alter total FAK protein levels (Figure 4A).

We also investigated the activity of the FAK signaling pathway by examining levels of phosphorylated FAK (p-FAK). It is well-established that activation of FAK results in the

autophosphorylation of Tyr397 which reveals a binding site for Src family kinases and mediates many of the downstream signaling events [37]. After treatment with 15d-PGJ_2 (0.3 μM for 30 min), p-FAK distribution is markedly altered whereby p-FAK is localized to the terminal ends of F-actin filaments in untreated cells and exposure to 15d-PGJ_2 results in a more diffuse and perinuclear pattern of p-FAK protein (Figure 4B). However, FAK phosphorylation assessed by Western blot analysis after treatment with 15d-PGJ_2 (0.3 μM, 15-30 min) showed no significant difference in p-FAK levels in whole cell lysates from 15d-PGJ_2 treated cells compared to vehicle control (result not shown). The total number of cells scoring positive for focal adhesions (> 6 focal adhesions/cell) was also quantified after treatment with 15d-PGJ_2. There was no difference in the number of cells scoring positive for focal adhesions after treatment with 15d-PGJ_2 (0.3 μM) for 30 min (data not shown); however, decreases in cells scoring positive for focal adhesions was evident after treatment for 4 h (Figure 4C), suggesting that treatment with 0.3 μM 15d-PGJ_2 induces focal adhesion disassembly.

It is clear that 15d-PGJ_2 can act through multiple mechanisms including redox signaling, PPARγ-dependent pathways, and the G protein-coupled prostaglandin D_2 receptor DP2 (reviewed in [38]). Interestingly, treatment with the DP2 agonist 15(R)-PGD_2 or the PPARγ agonist Rosiglitazone (ROSI) also resulted in a decrease in the number of cells scoring positive for focal adhesions (Figure 4C), while neither of these compounds altered cell motility (Supplementary Figure 3A,B). Given that 15d-PGJ_2 changes focal adhesion disassembly and p-FAK localization, with no significant change in total FAK, our results suggest that sub-lethal concentrations of 15d-PGJ_2 may alter FAK mediated signaling or localization. However, the fact that the focal adhesion disassembly caused by 15d-PGJ_2 can be recapitulated using PPARγ and DP2 agonists suggests that this effect is likely mediated through different mechanisms than those which mediate migration.

15d-PGJ_2 changes F-actin morphology

Since focal adhesions are the site at which the actin cytoskeleton is linked to the extracellular matrix [39], we investigated the effect of 15d-PGJ_2 on the F-actin cytoskeletal structure using Phalloidin. In the same samples which demonstrate p-FAK changes in response to 15d-PGJ_2 (Figure 4B), vehicle control treated cells exhibited a filamentous, elongated morphology of the F-actin cytoskeleton (Figure 4B, “EtOH” panel). However, treatment with 15d-PGJ_2 for 30 min caused extensive reorganization of the F-actin cytoskeleton resulting in rounding of the F-actin cytoskeleton (Figure 4B, “15d-PGJ_2” panel). The effects of PPARγ and DP2 agonists on the F-actin cytoskeleton were also examined. Neither ROSI nor 15(R)-PGD_2 had any gross effect on the F-actin cytoskeletal morphology (Supplementary Figure 3C) suggesting that the reorganization of the F-actin cytoskeleton in response to 15d-PGJ_2 does not occur through PPARγ or DP2-dependent pathways.

Concentration-dependent effect of bt-15d-PGJ_2 modification of actin and Keap1

It is well accepted that the actin cytoskeleton plays an important role in cellular migration [40]. It was previously shown that 15d-PGJ_2 can form covalent adducts with a number of important cytoskeletal components including actin, tubulin, and vimentin [2,3]. Moreover, 15d-PGJ_2 can affect cytoskeletal organization in neuroblastoma and mesangial cells [2,3]. We therefore sought to further characterize the effect of 15d-PGJ_2 on the F-actin cytoskeleton. In order to determine if 15d-PGJ_2 forms a direct adduct with actin at low concentrations, JC cells were treated with 0.3, 3, and 20 μM bt-15d-PGJ_2 for 4 h. Biotin-15d-PGJ_2 adducted proteins were then enriched from cell lysate protein using a neutravidin column. Total and bt-15d-PGJ_2-modified actin was detected by Western blotting. In Figure 5A, actin modification can be detected in cell lysates treated with 3 and 20 μM bt-15d-PGJ_2, consistent with reports in the literature of a direct modification of actin by 15d-PGJ_2 [2,41]. Importantly, minimal modification of actin was detected after 4h with 0.3 μM bt-15d-PGJ_2.

As a positive control, we compared actin adduct formation with another protein which is known to be adducted by 15d-PGJ_2, Kelch-like ECH-associated protein 1 (Keap1). Biotin-15d-PGJ_2 directly adducts Keap1 when cells are treated with 3 μM or 20 μM bt-15d-PGJ_2; however, minimal adduct formation on Keap1 was detected at 0.3 μM bt-15d-PGJ_2 (Figure 5A). The amount (%) of Keap1 and actin which were pulled down from the total cell lysate was assessed by calculating the quantity of each protein from the densitometry of the respective western blot and adjusting for amount of total protein loaded per lane. The amount of bt-15d-PGJ_2-modified Keap1 or actin was also measured in the eluate from the western blot by densitometry, and the percentage of each protein which was recovered by neutravidin pull-down from the total cell lysate protein is shown in Figure 5B (% modification). Cell lysate and pulled-down samples were analyzed and quantified from the same Western blot membrane in order to minimize variability from blotting development or exposure. While these experiments do not rule out the possibility that actin modification may occur in response to 15d-PGJ_2, they do suggest that 15d-PGJ_2 does not cause extensive actin modification or damage at very low concentrations which alter F-actin organization, focal adhesions, and migration.

Activation of EpRE-dependent intracellular antioxidants

It is known that modification of critical thiols in Keap1 by 15d-PGJ_2 results in an increase in activity of the transcription factor nuclear factor erythroid 2-related factor 2 (Nrf2), and subsequent transcription of genes under the control of the Electrophile Response Element (EpRE). Such genes include subunits of glutamyl cysteine ligase which controls the production of glutathione [4,42,43]. To demonstrate that adduct formation with Keap1 correlates with a biological response in JC cells, we monitored Keap1 modification by bt-15d-PGJ_2 and a subsequent increase in glutathione levels after 16 h.

Glutathione levels are significantly increased after exposure to 3 μM 15d-PGJ_2, but not at 0.3 μM (Figure 5C). Thus, these data demonstrate that adduct formation with Keap1 correlates with activation of EpRE-dependent gene expression in JC cells, but that this effect occurs at concentrations of 15d-PGJ_2 higher than those required to elicit focal adhesion turnover, attenuation of migration, or reorganization of the F-actin cytoskeleton.

Effects of p38 inhibition on 15d-PGJ_2-induced focal adhesion disassembly and F-actin cytoskeletal changes

Since direct modification of actin, PPARγ activation and DP2-dependent pathways cannot adequately account for the effects of 15d-PGJ_2 described herein, we investigated the role of a known redox active MAP kinase signaling pathway. The p38 pathway has been implicated in the regulation of actin dynamics and can be activated downstream of focal adhesion signaling [44-46]. Therefore, we assessed activation of p38 in response to low levels of 15d-PGJ_2 using Western blot analysis. Treatment with 15d-PGJ_2 (0.3 μM) for 15 and 30 min resulted in a significant increase in phosphorylated p38 (p-p38) compared to vehicle control (EtOH) treated cells (Figure 6A).

The effect of p38 inhibition on 15d-PGJ_2-induced alterations in focal adhesions and the F-actin cytoskeleton were next examined. There is a significant decrease (18%, $p < 0.01$) in the percentage of cells positive for focal adhesions upon treatment with 0.3 μM 15d-PGJ_2 (Figure 6B). The p38 inhibitor SB203580 alone had no effect on focal adhesions, but pretreatment with SB203580 for 30 min prevented the decrease in focal adhesion positive cells in response to 15d-PGJ_2 (Figure 6B).

JC cells were also pretreated with the p38 inhibitor SB203580**,** and then the effect of 15d-PGJ_2 on F-actin morphology was assessed. Figure 6C shows the F-actin cytoskeletal structure in JC cells that were pretreated with the p38 inhibitor prior to exposure to 0.24 μM BD-15d-

PGJ_2. Cells treated with the electrophile exhibited significant F-actin alterations. The p38 inhibitor itself had no apparent effect on the F-actin structure. Interestingly, pretreatment with SB203580 was able to prevent 15d-PGJ_2-induced F-actin cytoskeletal rounding. Taken together, these data suggest a role for the p38 pathway in the F-actin cytoskeletal reorganization and focal adhesion disassembly in response to 15d-PGJ_2. The effect of SB203580 on 15d-PGJ_2-induced attenuation of migration was also assessed; however, treatment with the p38 inhibitor itself resulted in the inhibition of migration (data not shown). It is, therefore, unclear what role p38 plays in mediating the effect of 15d-PGJ_2 on cellular migration.

DISCUSSION

Breast cancer metastasis is a major cause of mortality and morbidity in patients, and therefore agents which can inhibit this process, particularly with minimal toxicity to the patient, are desirable therapeutic options. In the studies presented here, we demonstrate that 15d-PGJ_2 at low concentrations (< 1 μM), which do not cause cytotoxicity, stimulates focal adhesion disassembly, causes F-actin reorganization, and attenuates migration of JC mouse mammary adenocarcinoma cells. Since these processes are required for successful metastasis, our data point to a potential anti-metastatic activity of 15d-PGJ_2.

This lipid electrophile can work through multiple mechanisms of action including post-translational modification of thiols, PPARγ, and DP2 receptors. It is for this reason that we examined the effects of PPARγ and DP2 agonists on the endpoints described herein. Rosiglitazone (ROSI), a PPARγ agonist, has previously been shown to alter focal adhesion signaling and impair migration [47]. Additionally, Powell [48] and Monneret [49,50] et al. demonstrated that 15d-PGJ_2 can bind to and activate the DP2 receptor on eosinophils. Though DP2 receptor expression seems to be limited to Type 2 helper T cells, cytotoxic T cells, eosinophils, and basophils in humans [51] while PPARγ is expressed more ubiquitously [52], we examined the effect of both DP2 and PPARγ agonists (15(R)-PGD_2 and ROSI, respectively) on focal adhesion disassembly. Both agonists were used at concentrations 20-fold higher than the reported EC_{50} for each compound [53,54], and both agonists had an effect on focal adhesions which was comparable to 15d-PGJ_2 (Figure 4C). Importantly, the effects on F-actin and migration appear to be independent of activation of PPARγ or the Prostaglandin D_2 receptor and direct modification of actin (Figures 5 and Supplementary Figure 3), but instead are likely to be modulated by one or more redox signaling pathways. It is expected that events upstream of these signaling pathways include the covalent modification of specific protein targets of 15d-PGJ_2, which have yet to be elucidated in this model.

There have been a number of previous studies demonstrating the ability of 15d-PGJ_2 to cause cancer cell death, and this is thought to occur primarily through PPARγ mediated activation of cell death pathways [23,47]. However, studies by our group and others have also shown that 15d-PGJ_2 causes apoptosis in a number of cell types, including endothelial cells, through the direct modification of protein thiols in mitochondrial proteins [55]. The modification of these protein leads to permeability transition and activation of apoptotic cell death [55]. This has raised the concern that 15d-PGJ_2 might have toxic side effects when used therapeutically at doses which kill cancer cells [56]. For this reason, we chose to investigate the possibility of targeting metastatic properties of cancer cells at concentrations of 15d-PGJ_2 which are not lethal. Our results demonstrate that cell processes which promote metastasis including migration, focal adhesion disassembly, and F-actin reorganization can be effectively modulated by low, sublethal concentrations of 15d-PGJ_2. Additionally, this is consistent with the finding that at low micromolar concentrations, 15d-PGJ_2 attenuates neutrophil migration after an inflammatory stimulus in a mouse model of peritonitis [27].

Our observation that 15d-PGJ_2 causes profound reorganization of the F-actin cytoskeleton (Figure 4B) is consistent with previous reports in neuroblastoma cells [3]. In their study, Aldini et al. attributed the F-actin changes to direct modification of actin by 15d-PGJ_2 through formation of covalent adducts [3]. In our study, we were able to recapitulate this result insomuch as direct protein adduct formation of 15d-PGJ_2 with actin was observed at 3 and 20 μM bt-15d-PGJ_2 (Figure 5A,B). Interestingly, bt-15d-PGJ_2 did not appreciably form protein adducts with actin at 0.3 μM, though there was still a profound effect on the F-actin cytoskeleton at this concentration. These results indicate that whereas 15d-PGJ_2 forms protein adducts with actin at higher concentrations, this adduct formation does not adequately explain the extensive effect on F-actin reorganization observed at low concentrations of 15d-PGJ_2 (< 1 μM).

Instead, we have focused on the p38 signaling pathway which is known to be redox regulated and has been implicated in actin structural dynamics in a number of cancer model systems [57]. The p38 signaling pathway was also recently shown to be activated by 15d-PGJ_2 at low micromolar concentrations in two human endothelial cell models [58,59]. Multiple stimuli that regulate the actin cytoskeleton, focal adhesion disassembly, cell motility, and invasion converge on the p38 signaling pathway. For example, in neuroblastoma cells, the WASP/WAVE family member WAVE3 has been shown to regulate actin polymerization and cytoskeletal organization through p38-dependent signaling [60]. Orr et al. also showed that focal adhesion disassembly in response to thrombospondin is regulated by p38 [61]. Furthermore, activation of Hsp27 by p38 is well established as an important regulator of actin polymerization and depolymerization [62]. Phorbol 12-myristate 13-actetate (PMA) induced migration of glioblastoma cells has been shown to occur through the p38/Hsp27 signaling axis [63]. More recently, it was shown that the motility of glioma cells is inhibited by flavonid silibinin by a mechanism involving ROS generation and p38 activation [64]. Together, these reports demonstrate the integral role p38 plays in modulating cytoskeleton organization, focal adhesion disassembly, motility, and invasion initiated by diverse stimuli. While our experiments implicate p38 in the mechanism of 15d-PGJ_2-mediated actin reorganization and focal adhesion disassembly (Figure 6), further studies are necessary to determine the role of other potentially important redox signaling pathways on this effect.

The mechanism by which 15d-PGJ_2 causes focal adhesion disassembly appears to be distinct from those responsible for migration and F-actin reorganization. FAK activation occurs primarily through integrin-mediated signal transduction. Downstream signaling events regulate multiple biological process including cell survival, proliferation, angiogenesis, and of particular interest in this context, migration and invasion (reviewed in [36]). Chen et al. previously demonstrated that 15d-PGJ_2 treatment of thyroid carcinoma cells caused decreased levels of the focal adhesion proteins vinculin, integrin β1, FAK, and paxillin; however, these effects were observed at concentrations of 15d-PGJ_2 which also caused cell death [47]. Focal adhesions have been shown to be modulated by a number of pathways including FAK, extracellular matrix components, and integrin signaling (reviewed in [36]). FAK signaling is altered in response to 15d-PGJ_2 not through changes in total FAK levels as previously described [47], but through changes in FAK signaling (Figure 4). Since PPARγ and DP2 agonists were able to decrease the number of cells which stain positive for focal adhesions to a similar extent as 15d-PGJ_2, it is likely that focal adhesion signaling is regulated by multiple mechanisms. Future studies will examine the role of signaling downstream of PPARγ and DP2 in the regulation of focal adhesion disassembly to determine if 15d-PGJ_2 activates common pathways.

In summary, we have shown that 15d-PGJ_2 attenuates mammary cancer cells motility at sublethal concentrations. This effect is preceded by extensive alterations in the F-actin cytoskeletal organization resulting in the rounding of the F-actin cytoskeleton and significant focal adhesion disassembly. Moreover, these effects appear to be independent of PPARγ

activation or the direct modification of actin by the electrophile. Our data indicate that the p38 signaling pathway plays an integral role in mediating the 15d-PGJ_2-induced alterations in the aforementioned parameters. While further studies are required to identify the redox-sensitive protein target or targets of 15d-PGJ_2 responsible for changes in F-actin, focal adhesions, and ultimately migration, it is clear that modulation of redox signaling pathways by electrophiles may constitute important anti-metastatic therapeutic avenues in the future.

Supplementary Material

Refer to Web version on PubMed Central for supplementary material.

Acknowledgments

FUNDING.

This study was supported by a Junior Faculty Development Grant from the Comprehensive Cancer Center at the University of Alabama at Birmingham (to AL), NIH R01 HL079644 to JEMU, NIH R01 CA87728 to DRW, and the National Foundation for Cancer Research (DRW). ARD is supported by T32 HL007918.

REFERENCES

1. Shiraki T, Kamiya N, Shiki S, Kodama TS, Kakizuka A, Jingami H. Alpha,beta-unsaturated ketone is a core moiety of natural ligands for covalent binding to peroxisome proliferator-activated receptor gamma. The Journal of biological chemistry 2005;280:14145–14153. [PubMed: 15695504]
2. Stamatakis K, Sanchez-Gomez FJ, Perez-Sala D. Identification of novel protein targets for modification by 15-deoxy-Delta12,14-prostaglandin J2 in mesangial cells reveals multiple interactions with the cytoskeleton. J Am Soc Nephrol 2006;17:89–98. [PubMed: 16291835]
3. Aldini G, Carini M, Vistoli G, Shibata T, Kusano Y, Gamberoni L, Dalle-Donne I, Milzani A, Uchida K. Identification of actin as a 15-deoxy-Delta12,14-prostaglandin J2 target in neuroblastoma cells: mass spectrometric, computational, and functional approaches to investigate the effect on cytoskeletal derangement. Biochemistry 2007;46:2707–2718. [PubMed: 17297918]
4. Levonen A-L, Landar A, Ramachandran A, Ceaser EK, Dickinson DA, Zanoni G, Morrow JD, Darley-Usmar VM. Cellular mechanisms of redox cell signalling: role of cysteine modification in controlling antioxidant defences in response to electrophilic lipid oxidation products. Biochem. J 2004;378:373–382. [PubMed: 14616092]
5. Oliva JL, Perez-Sala D, Castrillo A, Martinez N, Canada FJ, Bosca L, Rojas JM. The cyclopentenone 15-deoxy-Delta 12,14-prostaglandin J2 binds to and activates H-Ras. Proceedings of the National Academy of Sciences 2003;100:4772–4777.
6. Wu W-S. The signaling mechanism of ROS in tumor progression. Cancer and Metastasis Reviews 2006;25:695–705. [PubMed: 17160708]
7. Nelson KK, Melendez JA. Mitochondrial redox control of matrix metalloproteinases. Free Radical Biology and Medicine 2004;37:768–784. [PubMed: 15304253]
8. Kattan Z, Minig V, Leroy P, Dauça M, Becuwe P. Role of manganese superoxide dismutase on growth and invasive properties of human estrogen-independent breast cancer cells. Breast Cancer Research and Treatment. 2007
9. Ridnour LA, Oberley TD, Oberley LW. Tumor Suppressive Effects of MnSOD Overexpression May Involve Imbalance in Peroxide Generation Versus Peroxide Removal. Antioxidants & Redox Signaling 2004;6:501–512. [PubMed: 15130277]
10. Davis CA, Hearn AS, Fletcher B, Bickford J, Garcia JE, Leveque V, Melendez JA, Silverman DN, Zucali J, Agarwal A, Nick HS. Potent Anti-tumor Effects of an Active Site Mutant of Human Manganese-Superoxide Dismutase: EVOLUTIONARY CONSERVATION OF PRODUCT INHIBITION. J. Biol. Chem 2004;279:12769–12776. [PubMed: 14688256]
11. Iiizumi M, Liu W, Pai SK, Furuta E, Watabe K. Drug development against metastasis-related genes and their pathways: a rationale for cancer therapy. Biochimica et biophysica acta 2008;1786:87–104. [PubMed: 18692117]

12. Brown M, Cohen J, Arun P, Chen Z, Van Waes C. NF-kappaB in carcinoma therapy and prevention. Expert Opin Ther Targets 2008;12:1109–1122. [PubMed: 18694378]
13. Connor KM, Hempel N, Nelson KK, Dabiri G, Gamarra A, Belarmino J, Van De Water L, Mian BM, Melendez JA. Manganese superoxide dismutase enhances the invasive and migratory activity of tumor cells. Cancer Res 2007;67:10260–10267. [PubMed: 17974967]
14. Liebler DC. Protein damage by reactive electrophiles: targets and consequences. Chem Res Toxicol 2008;21:117–128. [PubMed: 18052106]
15. Satoh T, Lipton SA. Redox regulation of neuronal survival mediated by electrophilic compounds. Trends in Neurosciences 2007;30:37–45. [PubMed: 17137643]
16. Stamatakis K, Perez-Sala D. Prostanoids with Cyclopentenone Structure as Tools for the Characterization of Electrophilic Lipid-Protein Interactomes. Ann NY Acad Sci 2006;1091:548–570. [PubMed: 17341644]
17. Chaffer C, Thomas D, Thompson E, Williams E. PPARgamma-independent induction of growth arrest and apoptosis in prostate and bladder carcinoma. BMC Cancer 2006;6:53. [PubMed: 16519808]
18. Chen Y-X, Zhong X-Y, Qin Y-F, Bing W, He L-Z. 15d-PGJ2 inhibits cell growth and induces apoptosis of MCG-803 human gastric cancer cell line. World J Gastroenterol 2003;9:2149–2153. [PubMed: 14562367]
19. Cho W, Choi C, Park J, Kang S, Kim Y. 15-Deoxy-Δ12,14-prostaglandin J2 (15d-PGJ2) Induces Cell Death Through Caspase-independent Mechanism in A172 Human Glioma Cells. Neurochemical Research 2006;31:1247–1254. [PubMed: 17006759]
20. Fu Y-G, Sung JJY, Wu K-C, Bai AHC, Chan MCW, Yu J, Fan D-M, Leung WK. Inhibition of gastric cancer cells associated angiogenesis by 15d-prostaglandin J2 through the downregulation of angiopoietin-1. Cancer Letters 2006;243:246–254. [PubMed: 16412567]
21. Na H-K, Surh Y-J. Peroxisome proliferator-activated receptor [gamma] (PPAR[gamma]) ligands as bifunctional regulators of cell proliferation. Biochemical Pharmacology 2003;66:1381–1391. [PubMed: 14555212]
22. Nosjean O, Boutin JA. Natural ligands of PPAR[gamma]:: Are prostaglandin J2 derivatives really playing the part? Cellular Signalling 2002;14:573–583. [PubMed: 11955950]
23. Nunez NP, Liu H, Meadows GG. PPAR-[gamma] ligands and amino acid deprivation promote apoptosis of melanoma, prostate, and breast cancer cells. Cancer Letters 2006;236:133–141. [PubMed: 15979236]
24. Ceaser EK, Moellering DR, Shiva S, Ramachandran A, Landar A, Venkartraman A, Crawford J, Patel R, Dickinson DA, Ulasova E, Ji S, Darley-Usmar VM. Mechanisms of signal transduction mediated by oxidized lipids: the role of the electrophile-responsive proteome. Biochem Soc Trans 2004;32:151–155. [PubMed: 14748737]
25. Pignatelli M, Sanchez-Rodriguez J, Santos A, Perez-Castillo A. 15-Deoxy-{Delta}-12,14-prostaglandin J2 induces programmed cell death of breast cancer cells by a pleiotropic mechanism. Carcinogenesis 2005;26:81–92. [PubMed: 15485993]
26. Liu H, Zang C, Fenner MH, Possinger K, Elstner E. PPARγ Ligands and ATRA Inhibit the Invasion of Human Breast Cancer Cells in vitro. Breast Cancer Research and Treatment 2003;79:63–74. [PubMed: 12779083]
27. Napimoga MH, Vieira SM, Dal-Secco D, Freitas A, Souto FO, Mestriner FL, Alves-Filho JC, Grespan R, Kawai T, Ferreira SH, Cunha FQ. Peroxisome proliferator-activated receptor-gamma ligand, 15-deoxy-Delta12,14-prostaglandin J2, reduces neutrophil migration via a nitric oxide pathway. J Immunol 2008;180:609–617. [PubMed: 18097063]
28. Higdon AN, Dranka BP, Hill BG, Oh JY, Johnson MS, Landar A, Darley-Usmar VM. Methods for imaging and detecting modification of proteins by reactive lipid species. Free radical biology & medicine 2009;47:201–212. [PubMed: 19446632]
29. Spitz DR, Malcolm RR, Roberts RJ. Cytotoxicity and metabolism of 4-hydroxy-2-nonenal and 2-nonenal in H2O2-resistant cell lines. Do aldehydic by-products of lipid peroxidation contribute to oxidative stress? Biochem. J 1990;267:453–459. [PubMed: 2334404]

30. Tietze F. Enzymatic Method for Quantitative Determination of Nanogram Amounts of Total and Oxidized Glutathione: Applications to Mammalian Blood and Other Tissues. Analytical Biochemistry 1969;27:502–522. [PubMed: 4388022]
31. Murphy-Ullrich JE, Hook M. Thrombospondin modulates focal adhesions in endothelial cells. J. Cell Biol 1989;109:1309–1319. [PubMed: 2768342]
32. Moriai M, Tsuji N, Kobayashi D, Kuribayashi K, Watanabe N. Down-regulation of hTERT expression plays an important role in 15-deoxy-Delta12,14-prostaglandin J2-induced apoptosis in cancer cells. International journal of oncology 2009;34:1363–1372. [PubMed: 19360348]
33. Qiao L, Dai Y, Gu Q, Chan KW, Zou B, Ma J, Wang J, Lan HY, Wong BC. Down-regulation of X-linked inhibitor of apoptosis synergistically enhanced peroxisome proliferator-activated receptor gamma ligand-induced growth inhibition in colon cancer. Mol Cancer Ther 2008;7:2203–2211. [PubMed: 18645029]
34. Eichele K, Ramer R, Hinz B. Decisive role of cyclooxygenase-2 and lipocalin-type prostaglandin D synthase in chemotherapeutics-induced apoptosis of human cervical carcinoma cells. Oncogene 2008;27:3032–3044. [PubMed: 18071320]
35. Han H, Shin S-W, Seo C-Y, Kwon H-C, Han J-Y, Kim I-H, Kwak J-Y, Park J-I. 15-Deoxy-Δ12,14-prostaglandin J2 (15d-PGJ2) sensitizes human leukemic HL-60 cells to tumor necrosis factor-related apoptosis-inducing ligand (TRAIL)-induced apoptosis through Akt downregulation. Apoptosis 2007;12:2101–2114. [PubMed: 17786557]
36. Zhao J, Guan JL. Signal transduction by focal adhesion kinase in cancer. Cancer Metastasis Rev 2009;28:35–49. [PubMed: 19169797]
37. Cobb BS, Schaller MD, Leu TH, Parsons JT. Stable association of pp60src and pp59fyn with the focal adhesion-associated protein tyrosine kinase, pp125FAK. Mol. Cell. Biol 1994;14:147–155. [PubMed: 7505391]
38. Scher JU, Pillinger MH. 15d-PGJ2: the anti-inflammatory prostaglandin? Clinical immunology (Orlando, Fla 2005;114:100–109.
39. Hynes RO. Integrins: bidirectional, allosteric signaling machines. Cell 2002;110:673–687. [PubMed: 12297042]
40. Lambrechts A, Van Troys M, Ampe C. The actin cytoskeleton in normal and pathological cell motility. The International Journal of Biochemistry & Cell Biology 2004;36:1890–1909.
41. Gayarre J, Sanchez D, Sanchez-Gomez FJ, Terron MC, Llorca O, Perez-Sala D. Addition of electrophilic lipids to actin alters filament structure. Biochem Biophys Res Commun 2006;349:1387–1393. [PubMed: 16979589]
42. Tong KI, Kobayashi A, Katsuoka F, Yamamoto M. Two-site substrate recognition model for the Keap1-Nrf2 system: a hinge and latch mechanism. Biological chemistry 2006;387:1311–1320. [PubMed: 17081101]
43. Kobayashi M, Yamamoto M. Molecular mechanisms activating the Nrf2-Keap1 pathway of antioxidant gene regulation. Antioxid Redox Signal 2005;7:385–394. [PubMed: 15706085]
44. Pichon S, Bryckaert M, Berrou E. Control of actin dynamics by p38 MAP kinase - Hsp27 distribution in the lamellipodium of smooth muscle cells. J Cell Sci 2004;117:2569–2577. [PubMed: 15128872]
45. Korb T, Schluter K, Enns A, Spiegel H-U, Senninger N, Nicolson GL, Haier J. Integrity of actin fibers and microtubules influences metastatic tumor cell adhesion. Experimental Cell Research 2004;299:236–247. [PubMed: 15302590]
46. Hehlgans S, Haase M, Cordes N. Signalling via integrins: Implications for cell survival and anticancer strategies. Biochimica et Biophysica Acta (BBA) - Reviews on Cancer 2007;1775:163–180.
47. Chen Y, Wang SM, Wu JC, Huang SH. Effects of PPARgamma agonists on cell survival and focal adhesions in a Chinese thyroid carcinoma cell line. J Cell Biochem 2006;98:1021–1035. [PubMed: 16795079]
48. Powell WS. 15-Deoxy-delta12,14-PGJ2: endogenous PPARgamma ligand or minor eicosanoid degradation product? The Journal of clinical investigation 2003;112:828–830. [PubMed: 12975467]
49. Monneret G, Li H, Vasilescu J, Rokach J, Powell WS. 15-Deoxy-delta 12,14-prostaglandins D2 and J2 are potent activators of human eosinophils. J Immunol 2002;168:3563–3569. [PubMed: 11907120]

50. Monneret G, Cossette C, Gravel S, Rokach J, Powell WS. 15R-methyl-prostaglandin D2 is a potent and selective CRTH2/DP2 receptor agonist in human eosinophils. J Pharmacol Exp Ther 2003;304:349–355. [PubMed: 12490611]
51. Hirai H, Tanaka K, Yoshie O, Ogawa K, Kenmotsu K, Takamori Y, Ichimasa M, Sugamura K, Nakamura M, Takano S, Nagata K. Prostaglandin D2 selectively induces chemotaxis in T helper type 2 cells, eosinophils, and basophils via seven-transmembrane receptor CRTH2. J Exp Med 2001;193:255–261. [PubMed: 11208866]
52. Kliewer SA, Forman BM, Blumberg B, Ong ES, Borgmeyer U, Mangelsdorf DJ, Umesono K, Evans RM. Differential expression and activation of a family of murine peroxisome proliferator-activated receptors. Proc Natl Acad Sci U S A 1994;91:7355–7359. [PubMed: 8041794]
53. Cossette C, Walsh SE, Kim S, Lee GJ, Lawson JA, Bellone S, Rokach J, Powell WS. Agonist and antagonist effects of 15R-prostaglandin (PG) D2 and 11-methylene-PGD2 on human eosinophils and basophils. J Pharmacol Exp Ther 2007;320:173–179. [PubMed: 17041009]
54. Lehmann JM, Moore LB, Smith-Oliver TA, Wilkison WO, Willson TM, Kliewer SA. An antidiabetic thiazolidinedione is a high affinity ligand for peroxisome proliferator-activated receptor gamma (PPAR gamma). The Journal of biological chemistry 1995;270:12953–12956. [PubMed: 7768881]
55. Landar A, Shiva S, Levonen A-L, Oh J-Y, Zaragoza C, Johnson MS, Darley-usmar VM. Induction of the permeability transition and cytochrome c release by 15-deoxy-Delta12,14-prostaglandin J2 in mitochondria. Biochem J 2006;394:185–195. [PubMed: 16268779]
56. Ishihara S, Rumi MA, Okuyama T, Kinoshita Y. Effect of prostaglandins on the regulation of tumor growth. Current medicinal chemistry 2004;4:379–387. [PubMed: 15281909]
57. Cuenda A, Rousseau S. p38 MAP-Kinases pathway regulation, function and role in human diseases. Biochimica et Biophysica Acta (BBA) - Molecular Cell Research 2007;1773:1358–1375.
58. Józkowicz A, Nigisch A, Wegrzyn J, Weigel G, Huk I, Dulak J. Opposite effects of prostaglandin-J2 on VEGF in normoxia and hypoxia: role of HIF-1. Biochemical and Biophysical Research Communications 2004;314:31–38. [PubMed: 14715242]
59. Ho TC, Chen SL, Yang YC, Chen CY, Feng FP, Hsieh JW, Cheng HC, Tsao YP. 15-deoxy-Delta (12,14)-prostaglandin J2 induces vascular endothelial cell apoptosis through the sequential activation of MAPKS and p53. The Journal of biological chemistry 2008;283:30273–30288. [PubMed: 18718914]
60. Sossey-Alaoui K, Ranalli TA, Li X, Bakin AV, Cowell JK. WAVE3 promotes cell motility and invasion through the regulation of MMP-1, MMP-3, and MMP-9 expression. Experimental Cell Research 2005;308:135–145. [PubMed: 15907837]
61. Orr AW, Pallero MA, Murphy-Ullrich JE. Thrombospondin stimulates focal adhesion disassembly through Gi- and phosphoinositide 3-kinase-dependent ERK activation. The Journal of biological chemistry 2002;277:20453–20460. [PubMed: 11923291]
62. Dalle-Donne I, Rossi R, Milzani A, Di Simplicio P, Colombo R. The actin cytoskeleton response to oxidants: from small heat shock protein phosphorylation to changes in the redox state of actin itself. Free Radical Biology and Medicine 2001;31:1624–1632. [PubMed: 11744337]
63. Nomura N, Nomura M, Sugiyama K, Hamada J-I. Phorbol 12-myristate 13-acetate (PMA)-induced migration of glioblastoma cells is mediated via p38MAPK/Hsp27 pathway. Biochemical Pharmacology 2007;74:690–701. [PubMed: 17640620]
64. Kim KW, Choi CH, Kim TH, Kwon CH, Woo JS, Kim YK. Silibinin inhibits glioma cell proliferation via Ca2+/ROS/MAPK-dependent mechanism in vitro and glioma tumor growth in vivo. Neurochem Res 2009;34:1479–1490. [PubMed: 19263218]

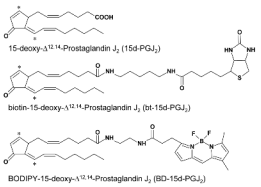

Figure 1. Structures of 15d-PGJ$_2$, BODIPY-15d-PGJ$_2$ and biotin-15d-PGJ$_2$
Electrophilic carbons are denoted by asterisks.

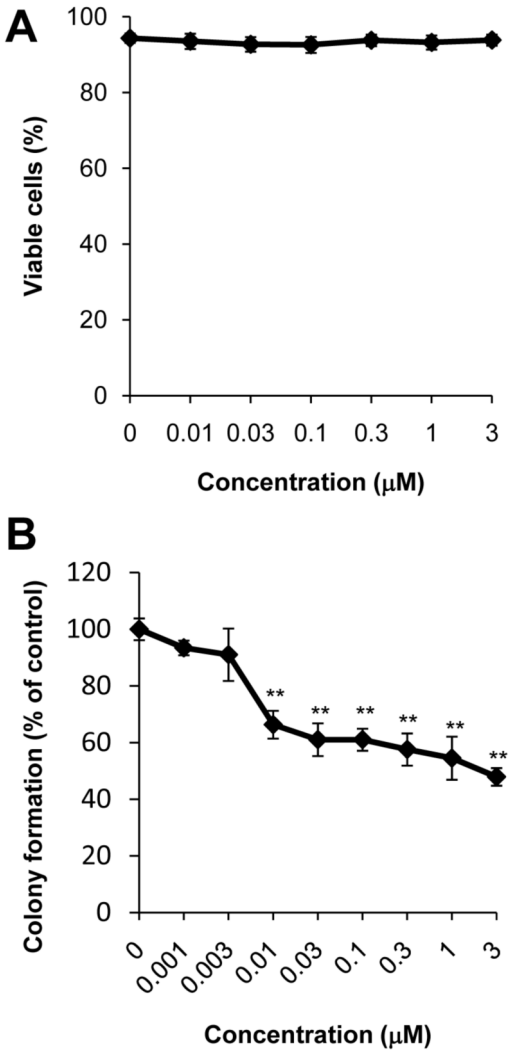

Figure 2. Effect of 15d-PGJ$_2$ on cell death and colony formation

The viability of JC cells treated with increasing concentrations of 15d-PGJ$_2$ (0.01-3 μM) for 16 h was assessed using PI and Annexin V flow cytometry (A). Cells which stained negative for both PI and Annexin V were scored as viable. Colony formation was also assessed after exposure to 15d-PGJ$_2$ and quantified (B). Ethanol was used as a vehicle control. Values shown represent means ± SEM, n = 3-9. ** $p < 0.01$ compared to vehicle control.

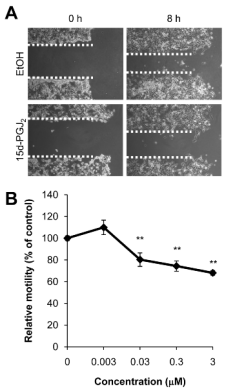

Figure 3. Effect of 15d-PGJ$_2$ on cell migration

JC cell migration was assessed using a scratch assay. Cells were treated with 15d-PGJ$_2$ (0.003-3 μM), and cell migration into cell-free area was assessed after 8 h. Representative images of 0.3 μM 15d-PGJ$_2$ treated wells (A) and quantification of dose response curve are shown (B). Ethanol (EtOH) was used as a vehicle control. Values represent means ± SEM, n = 3-12. ** $p < 0.01$ compared to vehicle control.

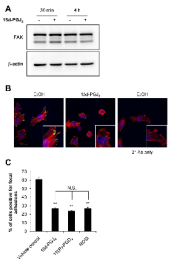

Figure 4. Effect of 15d-PGJ$_2$ on focal adhesion disassembly and migration

JC cells were treated with 15d-PGJ$_2$ (0.3 μM, 30 min or 4 h) and total FAK protein levels were determined by Western blot analysis. A representative Western blot image is shown (A). Phosphorylated FAK (p-FAK) was assessed in cells treated with 15d-PGJ$_2$ (0.3 μM, 30 min) using an anti-p-FAK antibody and a fluorophore-conjugated secondary antibody (green channel) and visualized using fluorescence confocal microscopy. Cells were co-stained with Alexa Fluor® 633 Phalloidin and DAPI to visualize F-actin (red channel) and nuclei (blue channel), respectively. Representative images of merged red, green, and blue channel are shown from samples prepared in triplicate (B). JC cells were also treated with 15d-PGJ$_2$ (0.3 μM), 15(R)-PGD$_2$ (0.24 μM), Rosiglitazone (ROSI, 2 μM) or vehicle control for 4 h then fixed in 3% glutaraldehyde. Focal adhesions were quantified using interference reflection microscopy. Values represent the mean percent of cells scored positive for focal adhesions (A). Ethanol (EtOH) was used as a vehicle control. Values represent means ± SEM, n = 9. ** $p < 0.01$ compared to vehicle control. N.S. signifies that no significant difference was observed.

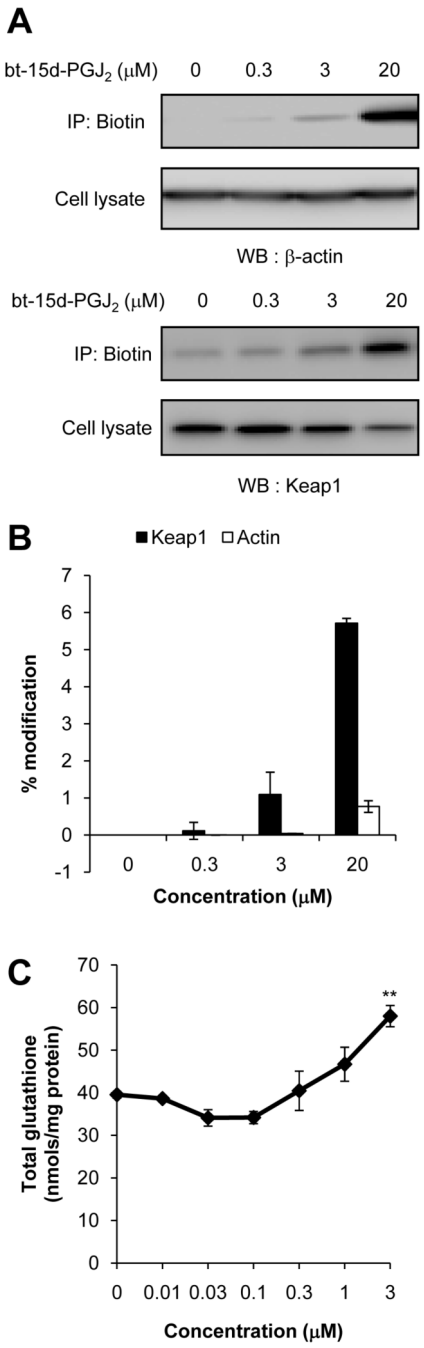

Figure 5. Dose-dependent adduct formation of bt-15d-PGJ$_2$ with β-actin and Keap1

JC cells were treated with 0.3, 3, and 20 μM bt-15d-PGJ$_2$ (4 h) and then biotinylated proteins were purified from cell lysates using a neutravidin column. β-actin or Keap1 were detected in cell lysate or eluent by Western blot analysis. Representative images are shown (A). The relative amount of β-actin or Keap1 which was affinity precipitated was determined by comparing the density of lanes containing cell lysate or eluate and correcting for protein loaded (B). Pull-down experiments were performed in duplicate, and values represent the mean ± range. As a read-out of Keap1 modification and subsequent Nrf2 activation, total glutathione was measured in lysates which were treated with 15d-PGJ$_2$ (0.1 - 3 μM, 16 h). Glutathione

levels were normalized to total lysate protein (C). Ethanol (EtOH) was used as a vehicle control. Glutathione values represent the mean ± SEM, n=3. ** $p < 0.01$ compared to vehicle control.

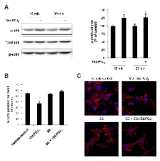

Figure 6. Role of p38 in focal adhesion disassembly and cytoskeletal arrangement regulation

JC cells were treated with 15d-PGJ_2 (0.3 μM, 15 and 30 min) or ethanol (EtOH) as a vehicle control and phosphorylated p38 (p-p38) was determined by Western blot analysis and quantified. A representative Western blot image is shown. Values represent the ratio of p-p38/total p38 normalized to time-matched vehicle control (A). JC cells were pretreated with the p38 inhibitor SB203580 ("SB"; 10 μM, 30 min), and then 15d-PGJ_2 (0.3 μM) was added for an additional 4 h. Cells were fixed in 3% glutaraldehyde and focal adhesions quantified using interference reflection microscopy. Values represent the mean percentage of cells scored positive for focal adhesions (B). JC cells were also pretreated with SB (10 μM, 30 min), and then BD-15d-PGJ_2 (0.24 μM) was added for an additional 30 min. Cells were then fixed, permeabilized and stained with 2 units of Alexa Fluor® 633 Phalloidin to visualize F-actin (red channel). Nuclei were visualized with DAPI (blue channel). Representative images of red and blue channel merged images are shown from samples prepared in triplicate. EtOH and DMSO were used as vehicle controls. (C). Values shown represent means ± SEM, n = at least 3-6. ** $p < 0.01$ compared to vehicle control.